Influence of a partially oxidized calcium cathode on the performance of polymeric light emitting diodes

G. G. Andersson, M. P. de Jong, F. J. J. Janssen, J. M. Sturm, L. J. van IJzendoorn,[a)]
A. W. Denier van der Gon, M. J. A. de Voigt, and H. H. Brongersma
Faculty of Applied Physics, Eindhoven University of Technology, Postbox 513, 5600 MB Eindhoven, The Netherlands

(Received 23 October 2000; accepted for publication 8 May 2001)

We investigated the influence of the presence of oxygen during the deposition of the calcium cathode on the structure and on the performance of polymeric light emitting diodes (pLEDs). The oxygen background pressure during deposition of the calcium cathode of polymeric LEDs was varied. Subsequently, the oxygen depth distribution was measured and correlated with the performance of the pLEDs. The devices have been fabricated in a recently built ultraclean setup. The polymer layers of the pLEDs have been spincoated in a dry nitrogen atmosphere and transported directly into an ultrahigh vacuum chamber where the metal electrodes have been deposited by evaporation. We used indium–tin–oxide as anode, OC_1C_{10} PPV as electroluminescent polymer, calcium as cathode, and aluminum as protecting layer. We achieved reproducibility of about 15% in current and brightness for devices fabricated in an oxygen atmosphere of $\ll 10^{-9}$ mbar. For further investigations the calcium deposition was carried out in an oxygen atmosphere from 10^{-8} to 10^{-5} mbar. We determined the amount of oxygen in the different layers of the current–voltage-light characterized pLEDs with elastic recoil detection analysis and correlated it with the characteristics of the devices. The external efficiency of the pLEDs decreases continuously with increasing oxygen pressure, the current shows a pronounced minimum. The brightness mostly decreases with increasing oxygen with an indication of a slight minimum. PLEDs with completely oxidized calcium are not operational. The first contact of the pLEDs with the dry glove box environment leads to an immediate reduction of current and brightness which is caused by the cooling of the devices by several degrees. Determining reproducible characteristics of pLEDs in the vacuum requires the measurement of their temperature. © *2001 American Institute of Physics.* [DOI: 10.1063/1.1383577]

I. INTRODUCTION

Polymeric light-emitting diodes (pLEDs) are fabricated under a broad range of conditions. The influence of the fabrication conditions on the characteristics of the pLEDs has been partially investigated, but full understanding has not been reached yet. In the fabrication process of pLEDs the low work function cathode is generally deposited by evaporation in a high vacuum system.[1–4] Unintentional impurities such as oxygen and moisture are present in a broad range of different concentrations. Commonly used materials for the cathodes are calcium or magnesium. The presence of oxygen and moisture will influence the work function of the cathode and thus the balance of the charge carrier or the chemical interaction of the low work function metal with the electroluminescent polymer. Bröms *et al.* found that an oxygen pressure of about 10^{-6} mbar during evaporation of the calcium cathode is necessary to achieve operational pLEDs using indium–tin–oxide (ITO) and calcium as electrodes and cyanosubstituted polyphenylenevinylene (CNPPV) as luminescent polymer,[5] while deposition of the calcium at lower pressures lead to device failure. Thus, the good performance of polymeric LEDs with calcium as cathode deposited under high vacuum conditions might be attributed to the presence of oxygen. Nevertheless, using magnesium as an electrode they achieved the best LEDs at the lowest oxygen pressure, i.e., at 10^{-10} mbar.[6] They also described the degradation of the structure of PPV due to photo-oxidation.[7] Böhler *et al.* found an increase of current, brightness, and efficiency in LEDs with a tris(8-hydroxyquinolinato) (Alq3) electroluminescent layer and magnesium cathode if the pressure during deposition of the cathode decreases to ultrahigh vacuum (UHV) conditions.[8] Summarizing, the influence on the presence of oxygen and moisture and the influence of the vacuum conditions during the deposition of magnesium and calcium cathodes has been partially investigated, but the correlation with the resulting modification of the structure of the LEDs and the reasons for the influence of the performance have not been found. However, it is of major interest for the fabrication process to know which vacuum conditions are necessary to archive the best performance of LEDs.

Recently, we built a setup for the fabrication of pLEDs under controlled conditions. Oxygen and moisture can be kept at a very low level during the fabrication and investigation of the LEDs. We investigated the influence of the presence of oxygen during the deposition of the calcium cathode on the structure and on the device characteristic of polymeric

[a)]Author to whom correspondence should be addressed; electronic mail: L.J.van.Ijzendoorn@tue.nl

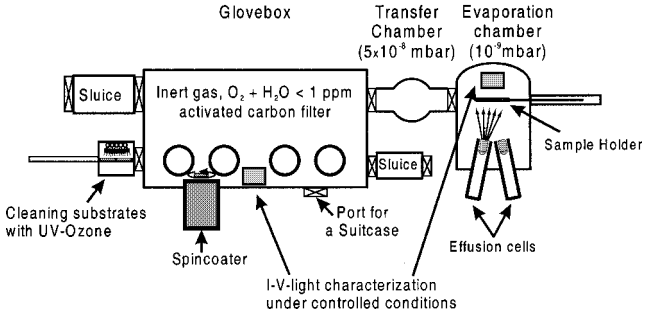

FIG. 1. Scheme of the LED production facility.

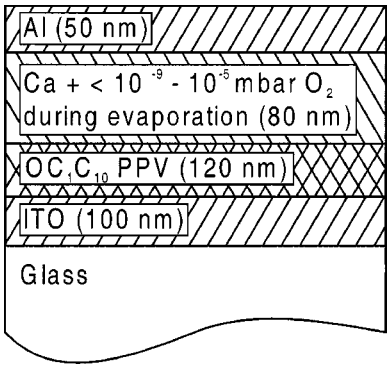

FIG. 2. Scheme of the investigated structure.

LEDs. Oxygen is expected to have a strong influence on the performance of LEDs using reactive low work function metals such as magnesium and calcium.

The influence of the presence of oxygen during the deposition of the calcium cathode was investigated by evaporating the calcium in an oxygen atmosphere of $10^{-8}-10^{-5}$ mbar. We determined both the current–voltage ($I-V$)-light characteristics and the concentration of oxygen. The concentration depth profiles have been determined with elastic recoil detection analysis (ERDA). We found a strong correlation between the presence of oxygen in the calcium cathode and the characteristics of the devices. The best LEDs were obtained with the lowest possible concentration of oxygen present during calcium evaporation.

II. EXPERIMENT

A. pLED fabrication and IV-light characterization

The devices are fabricated in a closed setup sketched in Fig. 1. Six devices can be fabricated at the same time under identical conditions. The setup consists of a glove box with less than 1 ppm oxygen and moisture, an UV-ozone pretreatment chamber and an UHV evaporation chamber. The setup is constructed such that samples may be transferred between the different chambers without exposure of the samples to air. The UV-ozone treatment is useful to remove hydrocarbons from the surface of ITO substrates.[9] The polymer layers are spin coated in the glove box, which is equipped with an activated carbon filter in order to remove the evaporated organic solvents. The window of the glove box is covered with a foil in order to prevent the polymers from the exposure to light of short wavelengths. The samples are introduced via a transfer chamber (base pressure of 5×10^{-8} mbar) into the UHV (base pressure of 1×10^{-9} mbar) chamber. The partial pressures in the UHV are measured with a residual gas analyzer Leybold Quadruvac Q 100 with a detection limit of $\sim10^{-9}$ mbar. The UHV chamber is equipped with an infrared lamp for soft bake of the organic layers. We can evaporate three different metals from commercial Riber ABN 135 L effusion cells. The layer thicknesses are determined with an Intellemetrics IL 150 quartz crystal monitor, which was calibrated with Rutherford backscattering spectrometry (RBS). The temperatures of the samples are measured during evaporation with NTC thermistors. IV-light characteristics of the LEDs can be measured either directly after fabrication in the UHV chamber or in the glove box. The brightness of the LEDs is determined with OPT301 photodiodes from Burr Brown which have been calibrated with a luminescence meter LS 110 from Minolta. The temperature of the samples during operation can be measured with NTCs and with a LUXTRON Fluoroptic thermometer. The temperature of the devices in the glove box is 23 ± 2 °C.

The LEDs or the half fabricates can be transported under dry nitrogen atmosphere to setups where the elemental composition of the surface and the bulk can be analyzed. For analysis of the surface we apply low energy ion scattering and x-ray photoelectron spectroscopy. For analysis of the bulk RBS, ERDA, and particle induced x-ray emission are applied.

We used ITO as the anode, a 130 nm thick layer of the electroluminescent polymer OC_1C_{10}-PPV as the emissive layer, 80 nm calcium as the cathode, and aluminum as the protecting layer. The glass/ITO substrates (100 nm ITO, 30 $\Omega/\square$, Merck) were cleaned in ultrapure acetone (Uvasol from Merck) and 2-propanol (Secsolv from Merck) each for 10 min in an ultrasonic bath. This wet cleaning step was followed by an UV-ozone treatment for 20 min. Directly after this treatment, the samples were transferred to the glove box with a dry nitrogen atmosphere without being exposed to air. The OC_1C_{10}-PPV layer was spin coated in the glove box from a 0.71 wt % toluene solution. The samples were transferred into an UHV evaporation chamber without having contact to air. The calcium cathode and aluminum protection layers were evaporated from effusion cells at temperatures of 510 and 1150 °C, respectively, the deposition rates at these temperatures are for calcium 4 Å/s and aluminum 1 Å/s. At a partial pressure of $<10^{-9}$ mbar oxygen the concentration of oxygen will be less than 0.1 at. % in the calcium layer at this deposition rate. Oxygen can be introduced into the UHV chamber by means of a leakage valve. The pressure during deposition of calcium was varied from less than 10^{-9} to 10^{-5} mbar. The fabrication of the devices was finished by evaporation of the aluminum layer. A scheme of the devices is shown in Fig. 2. 1 h after finishing the evaporation of the aluminum layer the devices have a temperature of 45 ± 2 °C. Within 15 h the equilibrium temperature in the UHV of about 28 ± 2 °C is reached.

From each set of LEDs we investigated oxygen and carbon concentration depth profiles with ERDA at cryogenic temperatures.

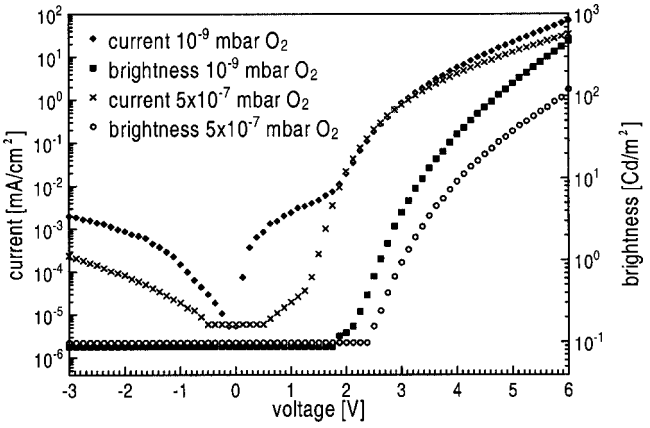

FIG. 3. $I-V$-light characteristics of LEDs with deposition of the calcium cathode in an oxygen pressure of $<10^{-9}$ and 5×10^{-7} mbar. The characteristics are measured in the glove box.

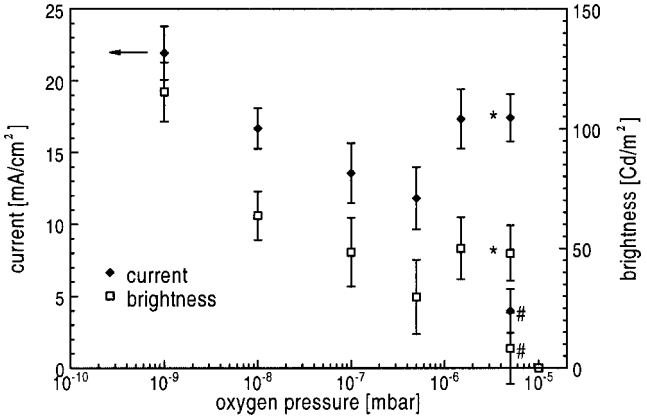

FIG. 4. Current and brightness for different partial pressures of oxygen at a bias of 5 V. 10^{-9} mbar means that no oxygen was let into the UHV chamber during deposition of the calcium, i.e., the oxygen pressure was some orders of magnitude lower than 10^{-9} mbar. At an oxygen pressure around 5×10^{-6} mbar the current and brightness of the devices changes rapidly with the pressure. Due to their position with respect to the oxygen inlet the samples marked with # experienced a somewhat higher oxygen pressure, and we attribute the difference between the groups thus to the high sensitivity of the device performance on the oxygen pressure in this range. Differences greater than 15% within one set of devices were observed only in this case, for all other experiments it was less than that.

B. Oxygen depth profiling with cryogenic ERDA

ERDA is a suitable method to determine concentration depth profiles of light elements such as carbon and oxygen up to a depth of approximately 1 μm. A depth resolution of 10 nm can be achieved. The pLEDs were transferred in dry nitrogen to our cryogenic RBS/ERDA setup.[10] This setup has been especially developed for RBS/ERDA analysis of organic samples, which are in general very sensitive to ion irradiation. Ion irradiation of organic materials leads to the formation of small volatile species along the ion track. Cooling the samples to cryogenic temperatures reduces drastically the mobility of these species. Measuring at room temperature would distort the concentration depth profiles, whereas the influence of the ion irradiation at cryogenic temperatures is negligible. In our cryogenic setup, the samples are cooled with a Gifford–McMahon cryocooler by APD cryogenics Inc, which has a cooling power of 2 W at 10 K. The sample temperature depends critically on the heat load transferred by the ion beam and the thermal contact between the samples and the cooler. For the experiments reported in this article the sample temperature is estimated as less than 30 K. At these conditions, damage suppression has been demonstrated successfully in Ref. 10.

The cryogenic ERDA measurements were performed using a 13.4 MeV He^{++} beam produced by our 2–30 MeV AVF cyclotron, taking advantage of a broad resonance in the $^4He(^{16}O,^{16}O)^4He$ scattering cross section at 13.4 MeV.[11] The recoil detection angle was set to 30° with respect to the ion beam; the angle between the sample normal and the ion beam was 70°. To discriminate between scattered He ions and recoiled C and O ions, pulse-shape discrimination[12] with low resistively passivated implanted planar silicon detectors[13] was applied.

III. RESULTS

The characteristic of a device without exposure to oxygen during calcium deposition is shown in Fig. 3. At a voltage of 5 V we achieve a current of 22 mA/cm^2 and a brightness of 115 Cd/m^2 in the glove box at device temperature of 23°. This corresponds to an external efficiency of 0.53 Cd/A. For devices that are prepared under comparable conditions, these current and brightness values are reproducible with an accuracy of 15% at bias voltages $\geqslant$4 V.

The characteristics of devices that were fabricated in an oxygen pressure $\geqslant10^{-8}$ mbar show a decrease of the brightness with increasing oxygen pressure, but the current is reduced only in a certain pressure regime. Current and brightness of the devices at a bias of 5 V are plotted in Fig. 4. The data points plotted at the x value of 10^{-9} mbar correspond to LEDs that were prepared without admitting oxygen to the UHV chamber during deposition of the calcium (10^{-9} mbar is the detection limit for oxygen for the residual gas analyzer). The oxygen pressure in an UHV system with the mentioned base pressure is usually about several orders of magnitude lower than 10^{-9} mbar. Each data point is an average over the six devices fabricated in one set. All error bars refer to the reproducibility of the device fabrication at $<10^{-9}$ mbar oxygen. The uncertainty within a set is somewhat smaller. For an oxygen pressure around 5×10^{-6} mbar a larger variance even within a single set of samples was observed and will be discussed later. The brightness decreases continuously from an oxygen pressure of $<10^{-9}$ mbar to 10^{-7} mbar by about a factor of 2.5. It possibly shows a minimum between 10^{-7} and 10^{-6} and drops to zero at a pressure of 1×10^{-5} mbar. The current reaches a minimum between 10^{-7} and 10^{-6} mbar and drops also to zero at a pressure of 1×10^{-5} mbar. The resulting external efficiency is plotted in Fig. 5. It decreases continuously from $<10^{-9}$ to 5×10^{-6} mbar, in total by about a factor of 2. At a pressure of 5×10^{-6} mbar the current and brightness of the devices changes rapidly with the pressure. This will be discussed below. At this pressure we found two different groups in the sets of six samples. Within both groups we found nearly identical results. The samples marked with* have been placed further from the oxygen inlet than the devices

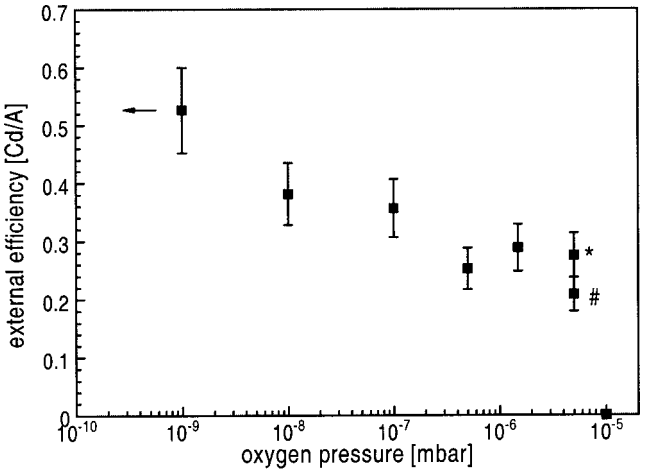

FIG. 5. External efficiency for different oxygen pressures at a bias of 5 V. For the data points at 10^{-9} mbar and the measurements marked with* and # holds the same as described in the caption of Fig. 4.

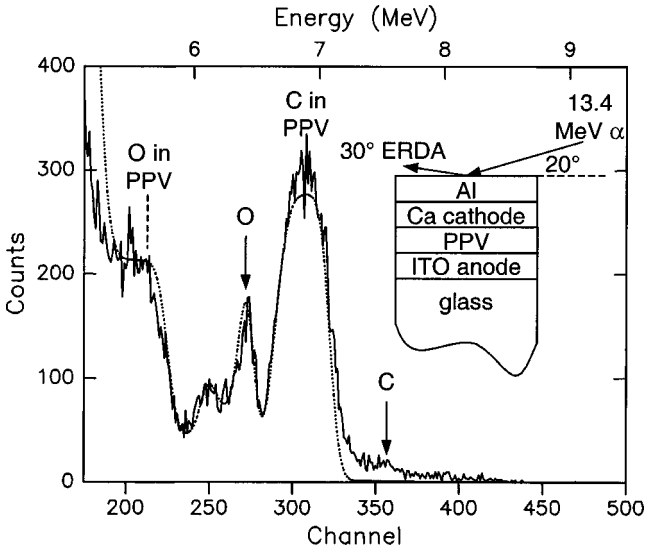

FIG. 6. ERDA spectrum (black curve) of an oxygen-free prepared pLED. The dotted curve represents the RUMP simulation. The energies of recoiled carbon (7.54 MeV) and (6.44 MeV) oxygen, present at the surface, are marked with arrows. Also indicated are the features of carbon and oxygen in the OC1C10-PPV film. The aluminum capping is partially oxidized, which results in the peak at the surface energy of oxygen. The small peak at about 6.1 MeV is due to calcium oxide at the interface between calcium and aluminum.

marked with #. The group marked with # had 4 times less current and 7 times less brightness compared with the other group. Due to their position with respect to the oxygen inlet the samples marked with # experienced a somewhat higher oxygen pressure, and we attribute the difference between the groups thus to the high sensitivity of the device performance on the oxygen pressure in this range. Differences greater than 15% within one set of devices were observed only in this case, for all other experiments it was less than that.

An ERDA measurement of a device with an oxygen pressure $<10^{-9}$ mbar during calcium deposition is shown in Fig. 6. The number of the recoiled particles is plotted against their energy which depends, among others, on the depth in the target from which they originate. The energy of the recoiled particle decreases with increasing mass and increasing depth.

The energies of recoiled carbon and oxygen, present at the surface, are marked in the spectrum. The feature between 6.8 and 7.1 MeV is due to carbon from the PPV. The step below 5.8 MeV results from oxygen in the PVV. The peaks at 6.44 and 6.1 MeV are thin oxide layers at the surface of the aluminum and at the interface of calcium and aluminum. In a large number of experiments slight variations (~30%) in the oxygen areal densities corresponding to the aluminum surface ($\sim 9\times10^{15}/\mathrm{cm}^2$) and calcium/aluminum interface ($\sim 5\times10^{15}/\mathrm{cm}^2$) have been observed. However, these variations did not significantly influence the $I-V$-light characteristics of the LEDs. Oxygen within the calcium layer causes signals between 5.8 and 6.1 MeV. The amount of oxygen in the calcium layer in Fig. 6 is less than 2%, which is the detection limit in this case. The ERDA spectra for the oxygen pressures of 10^{-7} and 5×10^{-6} mbar are shown in Fig. 7. We find an increasing amount of oxygen within the CaO_x layer with increasing oxygen pressure. The values of the amount of oxygen in the CaO_x layer determined by simulating the ERDA spectra with a modified version of the RUMP code are given in Fig. 8. The simulations are plotted in Figs. 6 and 7 as dotted lines. The maximum of the oxygen content (41 at. %) is almost reached at a pressure of 5×10^{-6} mbar,

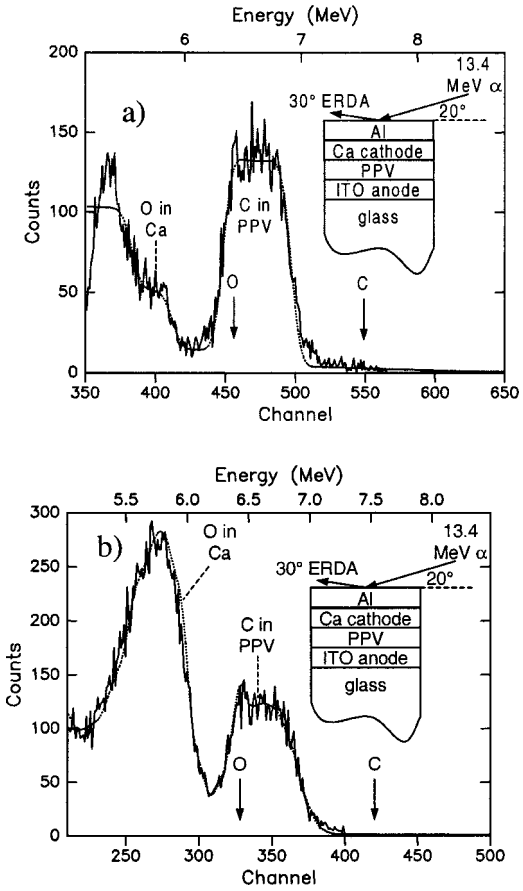

FIG. 7. ERDA spectrum (thin black line) of a pLED in which the calcium cathode was deposited in a background pressure of (a) 10^{-7} mbar and (b) 5×10^{-6} mbar of oxygen. The thick dotted line represents the RUMP simulation. The arrows indicate the energies of carbon (7.54 MeV) and oxygen (6.44 MeV) present at the surface. Also indicated are the features of carbon in the OC_1C_{10}-PPV film and oxygen in the calcium cathode.

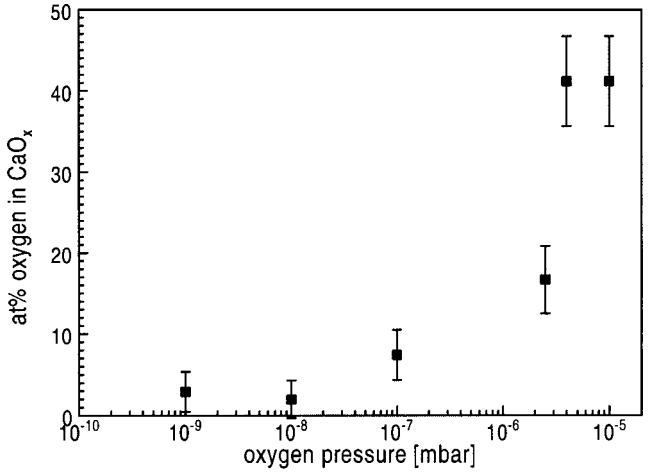

FIG. 8. Oxygen content in the calcium cathode. The amount of oxygen is determined from the simulations of the ERDA measurements.

where the LEDs are still operating. The failure of the devices at pressures $>5\times10^{-6}$ mbar is due to the fully oxidized and nonconducting CaO_x layer. Complete oxidation of calcium is reached at a flux ratio onto the surface of oxygen to calcium of ~3:1, assuming a sticking coefficient of 1 for the calcium in the evaporation process.

The onset voltage of the brightness is shown in Fig. 9. The onset voltage increases with increasing oxygen pressure until 5×10^{-7} mbar from a value of 2.1–2.3 V, as measured for the samples in the glove box.

All LEDs have been characterized in UHV within 1 h after their fabrication. The LEDs lose about a factor of 3 in current and brightness, when they are transferred from the UHV into the glove box. The time necessary for the transport is a few minutes. After the first contact with the glove box environment the LEDs keep the same characteristics after reintroduction into the UHV chamber as they exhibited in the glove box. The current and brightness due to the different environments at a voltage of 5 V are given in Fig. 10. The relative loss for both current and brightness is about a factor

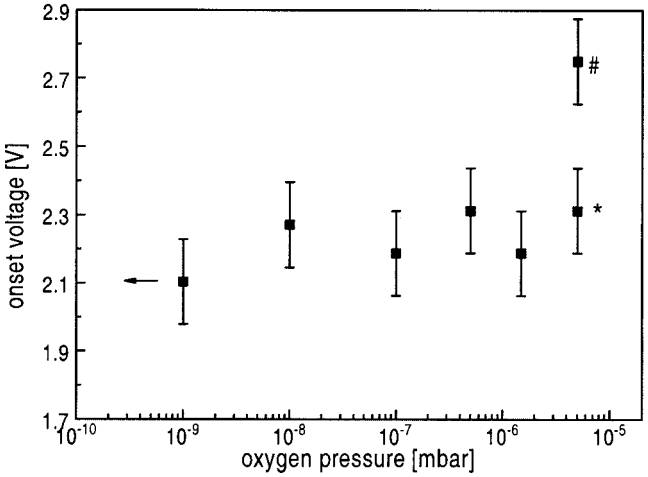

FIG. 9. Onset voltages of the brightness at different oxygen pressures. For the data points at 10^{-9} mbar and the measurements marked with* and # holds the same as described in the caption of Fig. 4.

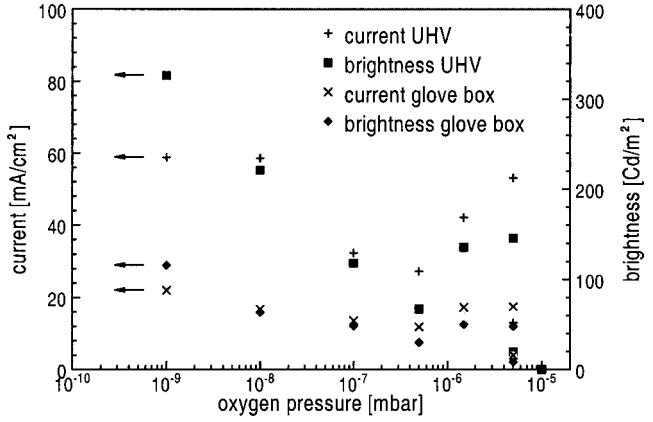

FIG. 10. Current and brightness before and after the first contact with the glove box atmosphere. For the data points at 10^{-9} and 5×10^{-6} mbar holds the same as described in the caption of Fig. 4.

of 3 and is independent of the oxygen partial pressure during the calcium deposition. Measurements of current and brightness at a constant voltage during operation of several hours within UHV and the glove box are shown in Fig. 11. In UHV the LEDs show a gradual decrease in current and brightness in the first 7 h. After that time the performance decreases only slightly within a total operation time up to 60 h. The LED in the glove box started at a lower current and brightness but shows only a slight decrease. The relative differences in current and brightness between operation in both environments remain constant after operation for 7 h at a factor of 1.5. Storage of the LEDs in UHV without operation also causes a loss of current and brightness but with a somewhat smaller factor than the operated LEDs. From Fig. 9 we also see that the onset voltage for the brightness is shifted to higher values by about 0.2 V. Further storage of the LEDs in the glove box does not change the performance of the LEDs significantly within 7 days.

IV. DISCUSSION

The current, brightness, and efficiency decrease with increasing oxygen pressure during deposition of the calcium cathode. We find a minimum in the current, a decrease of the

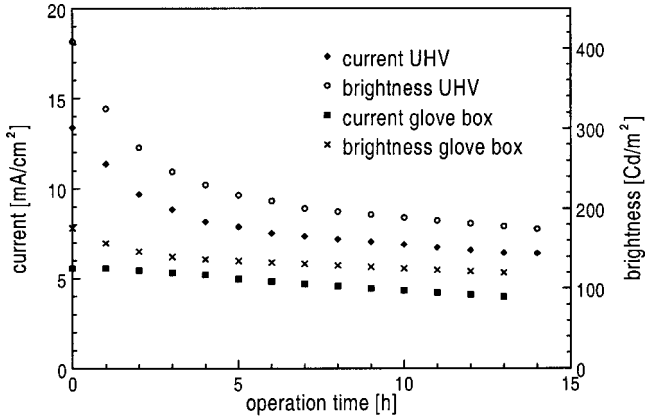

FIG. 11. Degradation of the LEDs during the first hours of operation in the UHV and in the glove box environment. The devices are both fabricated at an oxygen pressure $<10^{-9}$ mbar.

brightness possibly with a small minimum, a continuous loss of the efficiency, and an increase of the onset voltage of the brightness. It can be excluded that an increase of the resistance of the calcium layer with increasing oxygen content causes the changes of the characteristics. It can be shown that the $I-V$ curves of LEDs with different oxidized calcium cannot be shifted onto each other by correcting the applied voltage for an additional resistor in the CaO_x layer. Such a correction involves a voltage drop over the partially oxidized calcium layer which is proportional to the current, while the additional resistance of the CaO_x layer is kept constant for a certain LED.

Blom and de Jong developed a model for the charge transport in organic LEDs for the case that the current is not limited by injection barriers between the electrodes and the organic layer.[14] They showed that LEDs fabricated with the same materials and the same structure as we used have negligible injection barriers of less than 0.2 eV and that the current is dominated by hole transport. In their model the current is described as space charge limited with a temperature and field dependent mobility and a trap distribution for the electrons. The $I-V$ curves are fitted by determining numerically the field distribution, the charge carrier concentration, and the electron–hole recombination rate in the PPV layer. The $I-V$ characteristics with the lowest current—LEDs fabricated at 5×10^{-7} mbar and characterized in the glove box—are nearly identical to that published by Blom and de Jong in Ref. 14, which are space charge limited. All other LEDs showed a higher current and even a steeper increase of the current at a bias >3 V. Only for the set marked with # in Fig. 4 the current was lower. Thus, all the LEDs fabricated at oxygen pressures less than or approximately 5×10^{-6} mbar have a current which is space charge but not injection limited.

It seems plausible to explain the decrease of the current with a decrease of the injection of electrons because the cathode is modified. It can be expected that fewer electrons are injected from the oxidized calcium, e.g., due to a change of the work function. However, it should be noted that the devices still have I/V curves characteristic for space charge limited charge transport. Since the current shows a pronounced minimum at 5×10^{-7} the overall I/V behavior can be attributed only partially to a blocking of the electron injection with increasing oxygen pressure during deposition of the calcium. The reduction of the current simply due to blocking would not allow us to restore the current to the value of the unmodified cathode when the electron injecting electrode is nearly oxidized at 5×10^{-6} and must be attributed to other effects. Since the holes are the major charge carriers, a decrease of the current upon oxygen exposure must be also due to either a change in the hole mobility or to a change in the trap distribution of the holes and thus of the charge carrier concentration and the field distribution in the polymer layer. A plausible explanation is that the decrease of the current for oxygen pressures $<10^{-7}$ mbar is induced by oxidation of calcium in the CaO_x/PPV interface region. For oxygen background pressures near 5×10^{-6} mbar the calcium is nearly oxidized during the deposition process. The mobility of an oxidized calcium atom is probably lower than that of an unoxidized atom which hinders the diffusion of the, calcium into the PPV. This might lead to a sharpening of the CaO_x/PPV interface by suppression of the diffusion of individual calcium atoms or ions into the PPV. As a consequence the trap distribution of holes near the interface associated with calcium is altered (probably lowered) which will increase the hole current.

The brightness of the devices decreases more strongly than the current with increasing oxygen pressure, which results in a decreasing efficiency. A reason for the decrease of the brightness could be a decrease of the area of the PPV/CaO_x interface, from which electrons can be injected. If calcium oxide would grow in islands, the interface of the PPV with CaO_x would consist of small areas of fully and of unoxidized calcium. The fully oxidized islands will be insulating and charges would be injected only from the areas where the calcium is not oxidized. As a result, the active area of the LEDs would be reduced. However, since calcium is very reactive with oxygen, it is very unlikely that the oxygen atoms will move over the calcium surface in order to form islands of fully oxidized calcium, instead the oxygen will be chemisorbed immediately.

The decrease of the brightness can be explained, in our opinion, by assuming that the electron injection from the cathode is reduced. The reason could be a reduction of the work function of the partially oxidized calcium, which would also explain an increase of the onset voltage of the brightness. The increase of the work function could be accompanied by the creation of electron traps at the PPV CaO_x interface caused by the partially oxidized PPV, which decreases the current of electrons into the recombination zone of electrons and holes and thus decreases the brightness.

The decrease in current and brightness during storage in the UHV and during the transport from the UHV to the glove box can be explained very well with the change in the temperature of the devices and thus the change of the mobility of the charge carriers using the parameter published by Blom and de Jong.[14]

V. CONCLUSIONS

In our setup we are able to fabricate LEDs with a high reproducibility. We have correlated the oxygen pressure during the deposition of the calcium cathode with the changes in the structure of the LEDs and the performance of the devices by determining oxygen concentration depth profiles with cryogenic ERDA of characterized LEDs. The best LEDs are obtained at an oxygen pressure $<10^{-9}$ mbar, which is in contradiction to the results from Salaneck and co-workers.[7] This may be due to different preparation conditions before depositing the calcium electrode, e.g., by spin coating the PVV in air, which would result in a partially oxidized PPV. It could be also due to differences in the chemical structure of the used PPV. Comparing our results with those published by Blom and de Jong show, that the performance of LEDs is significantly affected by the residual gas present during the deposition of the calcium electrode in a high vacuum system.

We showed that the presence of oxygen during calcium deposition results in a decrease in brightness and efficiency.

The degradation process is attributed to the blocking of the electron injection and a decrease in hole mobility close to the PPV/CaO_x interface, to an increase in work function of the partially oxidized PPV or the creation of traps.

After correction of the $I-V$-light behavior of the devices as measured in the UHV chamber for the difference in temperatures, we find that device performance after transport into the glove box is virtually the same as measured in the UHV chamber directly after preparation. This shows that the devices after preparation are not influenced by the remaining impurities in the glove box, i.e., water and oxygen levels up to 1 ppm. Consequently, in our opinion, the device performance as measured in the glove box is characteristic for the intrinsic properties of the materials used in these devices.

However, it should be kept in mind that it cannot fully be excluded that during the whole processing and characterizing of the LEDs in the glove box impurities on a very low level can be incorporated in the devices, e.g., during spin coating of the polymer layer, and still have a small influence on device performance. Only for devices which can be prepared fully under UHV conditions, e.g., by evaporation of the organic layer in the UHV chamber (only feasible for certain oligomers), will it be possible to rule out completely the effect of such impurities.

For the future we plan to model the $I-V$-light characteristics and to measure hole and electron mobilities in order to determine more precisely the reasons, which cause the described effects.

ACKNOWLEDGMENTS

This work has been sponsored by grants from the Dutch Foundation for Fundamental Research (FOM) and the Priority Program Materials of the Organization for Scientific Research (PPM-NWO).

[1] J. S. Kim, M. Granström, R. H. Friend, N. Johansson, W. R. Salaneck, R. Daik, W. J. Feast, and F. Cacialli, J. Appl. Phys. **84**, 6859 (1998).
[2] F. Steuber, J. Staudigel, M. Stössel, J. Simmerer, and A. Winnacker, Appl. Phys. Lett. **74**, 3558 (1999).
[3] J. C. Scott, J. H. Kaufman, P. J. Brock, R. DiPietro, J. Salem, and J. A. Goitia, J. Appl. Phys. **79**, 2745 (1996).
[4] S. Karg, M. Meier, and W. Riess, J. Appl. Phys. **82**, 1951 (1997).
[5] P. Bröms, J. Birgersson, N. Johansson, M. Lögdlund, and W. R. Salaneck, Synth. Met. **74**, 179 (1995).
[6] P. Bröms, J. Birgerson, and W. R. Salaneck, Synth. Met. **88**, 255 (1997).
[7] K. Z. Xing, N. Johansson, G. Beamson, D. T. Clark, J.-L. Brédas, and W. R. Salaneck, Adv. Mater. **9**, 1027 (1997).
[8] A. Böhler, S. Dirr, H.-H. Johannes, D. Ammermann, and W. Kowalsky, Synth. Met. **91**, 95 (1997).
[9] S. K. So, W. K. Choi, C. H. Cheng, L. M. Leung, and C. F. Kwong, Appl. Phys. A: Mater. Sci. Process. **68**, 447 (1999).
[10] M. P. de Jong, L. J. van IJzendoorn, and M. J. A. de Voigt, Nucl. Instrum. Methods Phys. Res. B **161–163**, 207 (2000).
[11] M. K. Mehta, W. E. Hunt, and R. H. Davis, Phys. Rev. **160**, 791 (1967).
[12] S. S. Klein and H. A. Rijken, Nucl. Instrum. Methods Phys. Res. B **66**, 395 (1992).
[13] Canberra Semiconductor N. V. (www.canberra.com), B-2250 Olen, Belgium.
[14] P. W. Blom and M. J. M. de Jong, IEEE J. Sel. Top. Quantum Electron. **4**, 105 (1998).